Contribution from the Dipartimento di Chimica Inorganica
e Struttura Molecolare, Università di Messina, 98100 Messina, Italy

Synthesis and NMR Investigation of Dirhodium(4+) Formamidinate Complexes Containing 2-(Diphenylphosphino)pyridine as a Bridging Ligand. X-ray Crystal Structure of the Complex $Rh_2(form)_2(\mu\text{-}PPh_2Py)_2(O_2CCF_3)_2$ (form = *N*,*N*'-Di-*p*-tolylformamidinate)

Enrico Rotondo, Giuseppe Bruno, Francesco Nicolò, Sandra Lo Schiavo, and Pasquale Piraino*

Received April 3, 1990

The Rh_2^{4+} complex $Rh_2(form)_2(O_2CCF_3)_2(H_2O)_2$ (form = *N*,*N*'-di-*p*-tolylformamidinate) reacts with 2-(diphenylphosphino)-pyridine in molar ratios 1:1 and 1:2, giving the complexes $Rh_2(form)_2(\mu\text{-}O_2CCF_3)(\mu\text{-}PPh_2Py)(O_2CCF_3)$ (**1**) and $Rh_2(form)_2(\mu\text{-}PPh_2Py)_2(O_2CCF_3)_2$ (**2**), respectively. The complexes were characterized by IR and ^1H and ^{31}P NMR spectroscopy. Both complexes exhibit a "lantern" type structure with the axial sites occupied by one or two monoligated trifluoroacetate groups, respectively. Complex **2** was also characterized by single-crystal X-ray diffraction analysis, crystallizing in the monoclinic space group $P2_1/n$, with a = 19.608 (2) Å, b = 19.384 (2) Å, c = 20.576 (3) Å, β = 117.16 (3)°, V = 6958.34 Å^3, Z = 4, d_c = 1.343 g/cm^3. The two phosphorus ligands are observed in a cisoid arrangement, head-to-tail fashion. The Rh–Rh bond distance [2.5406 (6) Å] is appreciably greater than those observed in other formamidinate derivatives as consequence of the P···N separation. Conductivity measurements indicate that in acetonitrile solution the monoligated trifluoroacetate groups dissociate, giving rise to the cationic species $[Rh_2(form)_2(\mu\text{-}O_2CCF_3)(\mu\text{-}PPh_2Py)]^+$ (**3**) and $[Rh_2(form)_2(\mu\text{-}PPh_2Py)_2]^{2+}$ (**5**) that were isolated by reacting acetonitrile solutions of **1** and **2** with $TlPF_6$. The same experiment carried out in acetone gives the monocationic complex $[Rh_2(form)_2(\mu\text{-}PPh_2Py)_2(O_2CCF_3)]PF_6$ (**4**). The monoligated trifluoroacetate groups of **1** and **2** are displaced by halide ions, giving the complexes $Rh_2(form)_2(\mu\text{-}O_2CCF_3)(\mu\text{-}PPh_2Py)X$ (X = Cl (**6**), Br (**7**)), $Rh_2(form)_2(\mu\text{-}PPh_2Py)_2(O_2CCF_3)Cl$ (**8**), and $Rh_2(form)_2(\mu\text{-}PPh_2Py)_2I_2$ (**9**). The reactions between $Rh_2(form)_2(O_2CCF_3)_2(H_2O)_2$ and PPh_2Py, molar ratios 1:1 and 1:2, have been also investigated by ^{31}P NMR spectroscopy. The ^{31}P NMR spectra in $CDCl_3$ at 225 K of the 1:1 mixture reveal the quasi-quantitative formation of a monoaxial adduct together with small quantities of bisaxial adduct. On warming of solutions to 310 K, the monoadduct isomerizes to give a mixture of equatorial isomers. The same experiments carried out in acetonitrile lead to the formation of only one isomer. When the experiment is performed with the ratio of 1:2, the ^{31}P NMR spectra, recorded at 225 K, show the formation of a bisadduct (δ_P = −96.05) that, on warming to 310 K, isomerizes to give an equatorial isomer that exhibits a broad doublet centered at δ 29.01. Both the 1:1 and 1:2 equatorial adducts are stable and do not undergo transformation into the axial isomers upon cooling the samples at 225 K.

Recently, we have reported the NMR investigation of the Rh_2^{4+} complex $Rh_2(form)_2(O_2CCF_3)_2(H_2O)_2$ (form = *N*,*N*'-di-*p*-tolylformamidinate) in the presence of monodentate phosphorus ligands.[1] The formation of axial monoadducts (class I) was observed at 225 K whereas at 308 K a mixture of axial and equatorial (class II) adducts was formed, the ratio depending on the bulk of the phosphine used. With the bulkiest tertiary phosphines, PPh_3 and $P(C_6H_{11})_3$, only equatorial adducts were obtained. The IR and ^1H, ^{13}C, ^{19}F, and ^{31}P NMR data did not allow the unambiguous assignment of the structure of these bent isomers, and the attempts to grow X-ray diffraction quality crystals failed. Nevertheless, we suggested that the isomerization from the linear to the bent conformation involves breaking of one Rh–O bond and consequent formation of complex **1a** according to the mechanism in Scheme I. However, breaking of the Rh–N bond of one Rh–N–C–N–Rh ring with formation of complex **2a** cannot be ruled out.

To obtain additional support for the above suggestion, we investigated the interaction of the complex $Rh_2(form)_2(O_2CCF_3)_2(H_2O)_2$ with the "small-bite" bidentate ligand 2-(diphenylphosphino)pyridine (PPh_2Py) in the hope that its tendency to act as a bridging ligand could lead to complete displacement of one trifluoroacetate or formamidinate group from the equatorial position. In this paper we report on the NMR investigation of the above-cited complex with PPh_2Py in various molar ratios. We report also full details of the synthesis, characterization, and reactivity pattern of the mixed-ligand Rh_2^{4+} complexes $Rh_2(form)_2(\mu\text{-}O_2CCF_3)(\mu\text{-}PPh_2Py)(O_2CCF_3)$ (**1**) and $Rh_2(form)_2(\mu\text{-}PPh_2Py)_2(O_2CCF_3)_2$ (**2**), in which one or both the trifluoroacetate groups are axially monocoordinated. The X-ray analysis of complex **2** supports the proposed structure.

The objectives of this paper are 2-fold, first, to support the mechanism proposed for the isomerization from the linear to the bent isomer of the PPh_3 or PCy_3 monoadducts and, second, to provide further arguments for the statement that ligands neutral or nonisoelectronic with the carboxylate ions can support the Rh_2^{4+} core.[2]

Experimental Section

Materials. $Rh_2(form)_2(O_2CCF_3)_2(H_2O)_2$[3] and 2-(diphenylphosphino)pyridine[4] were prepared according to literature procedures. Other spectra and solvents were used as received. Infrared spectra were recorded on KBr pellets with a Perkin-Elmer FT 43 instrument. The ^1H and ^{31}P NMR spectra were measured in $CDCl_3$ by using a Bruker WP-80SY spectrometer. The chemical shifts are referenced to Me_4Si for ^1H and external 85% H_3PO_4 for ^{31}P (high frequency is taken as being positive). Elemental analyses were performed by the Microanalytical Laboratory of the Organic Chemistry Institute of Milan and Analitische Laboratorien Malissa and Reuter, Elbach, West Germany.

Synthesis of $Rh_2(form)_2(\mu\text{-}O_2CCF_3)(\mu\text{-}PPh_2Py)(O_2CCF_3)$ (1). To a diethyl ether solution (15 mL) of $Rh_2(form)_2(O_2CCF_3)_2(H_2O)_2$ (0.2 g, 0.21 mmol) was added 0.057 g (0.21 mmol) of solid PPh_2Py. The reaction mixture immediately changes from light to dark green and then slowly to red-orange. After 2 h the reaction mixture consisted of a light brown solid suspended in a red-orange solution. The solid was collected by filtration, washed with three 5-mL portions of cold ether, and dried in vacuo. Crystallization from CH_2Cl_2/*n*-heptane gives red crystals. Yield: 87%. Anal. Calcd for $C_{51}H_{44}N_5F_6PRh_2O_4$: C, 53.64; H, 3.88; N, 6.13; P, 2.71. Found: C, 53.38; H, 4.02; N, 5.71; P, 3.30. Molar conductivity (Ω^{-1} cm^2 M^{-1}): λ 106 (CH_3CN, 10^{-3} M), 118 (CH_3CN, 10^{-4} M), 12 ($C_6H_5NO_2$, 10^{-4} M). Infrared spectrum (cm^{-1}): (KBr pellet) ν(N=C=N) 1565 (vs); $\nu_{asym}(CO_2)$ 1635 (vs), 1687 (m), 1701 (m); (CH_3CN) $\nu_{asym}(CO_2)$ 1695 (s).

Synthesis of $Rh_2(form)_2(\mu\text{-}PPh_2Py)_2(O_2CCF_3)_2$ (2). Crude PPh_2Py (0.23 g, 0.88 mmol) was added to a stirred solution of $Rh_2(form)_2(O_2CCF_3)_2(H_2O)_2$ (0.2 g, 0.21 mmol) in diethyl ether (30 mL). The solution changed rapidly to a dark green and then slowly to a yellow-red color. Stirring of the mixture was continued for 3 h whereupon a brown precipitate also formed. After removal of the solvent via a syringe, the residue was repeatedly washed with diethyl ether (4 × 15 mL) to remove the unreacted phosphine and crystallized from $CHCl_3$/*n*-heptane. Yield:

(1) Rotondo, E.; Mann, B. E.; Piraino, P.; Tresoldi, G. *Inorg. Chem.* **1989**, *28*, 3070.

(2) Cotton, F. A.; Dunbar, K. R.; Verbruggen, M. G. *J. Am. Chem. Soc.* **1987**, *109*, 5498.

(3) Piraino, P.; Bruno, G.; Tresoldi, G.; Lo Schiavo, S.; Zanello, P. *Inorg. Chem.* **1987**, *26*, 91.

(4) Mann, F. G.; Watson, J. *J. Org. Chem.* **1948**, *13*, 502.

0020-1669/91/1330-1195$02.50/0

Scheme I

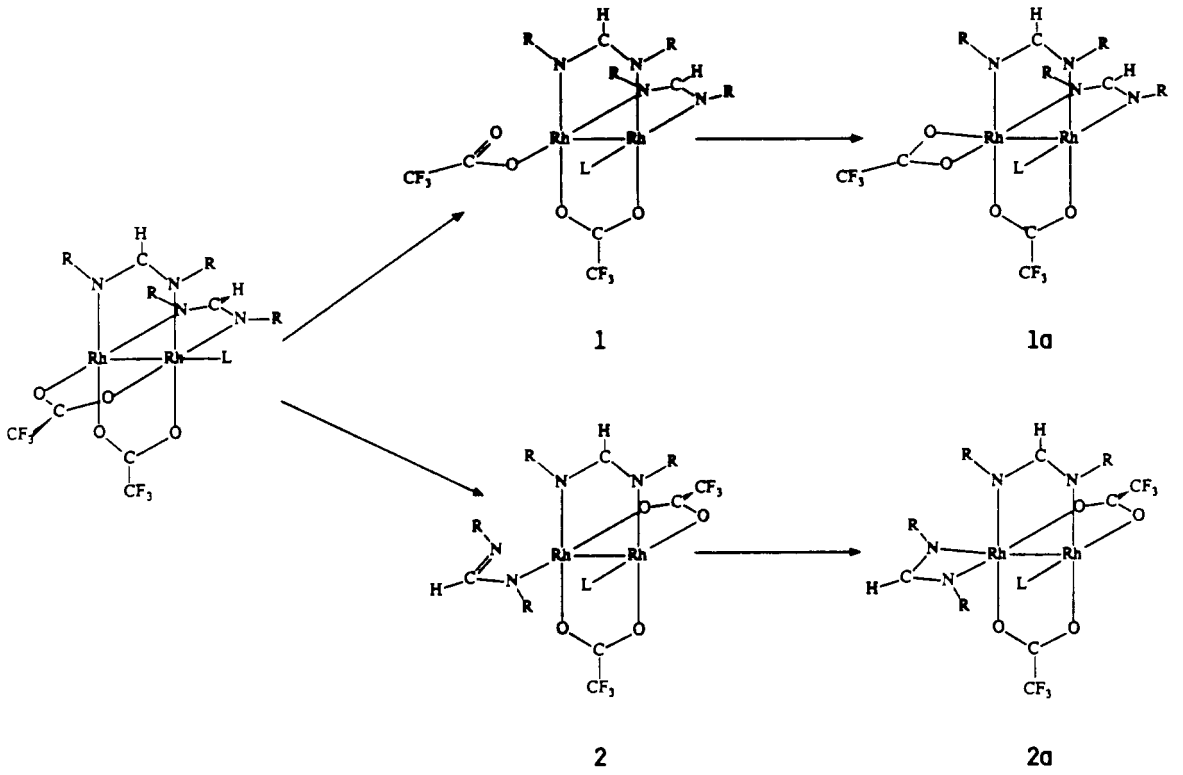

78%. Anal. Calcd for $C_{68}H_{58}N_6O_4F_6P_2Rh_2 \cdot CHCl_3$: C, 55.65; H, 3.99; N, 5.64; P, 4.16; F, 7.65. Found: C, 55.60; H, 4.14; N, 5.59; P, 3.77; F, 7.83. Molar conductivity (Ω^{-1} cm^2 M^{-1}): λ 296 (CH_3CN, 10^{-4} M), 235 (CH_3CN, 10^{-3} M), 78 (acetone, 10^{-3} M), 23 ($C_6H_5NO_2$, 10^{-4} M), 71 (CH_3OH, 10^{-4} M), 23.5 (CH_2Cl_2, 10^{-4} M). Infrared spectrum (cm^{-1}): (KBr pellet) ν(N=C=N) 1562 (s); $\nu_{asym}(CO_2)$ 1663 (vs), 1683 (sh); (CH_3CN) $\nu_{asym}(CO_2)$ 1696 (vs); (CH_2Cl_2) $\nu_{asym}(CO_2)$ 1683 (vs, br).

Synthesis of $[Rh_2(form)_2(\mu\text{-}O_2CCF_3)(\mu\text{-}PPh_2Py)]PF_6$ (3). A CH_3CN solution of **1** (0.13 g, 0.11 mmol) was treated with an excess of $TlPF_6$ (0.1 g, 0.28 mmol), and the mixture was stirred at room temperature for 3 h. After filtration the solvent was removed in vacuo and the orange residue washed with diethyl ether. Orange crystals were obtained by crystallization from benzene/*n*-heptane. Yield: 38%. Anal. Calcd for $C_{49}H_{44}N_5F_9P_2O_2Rh_2$: C, 50.14; H, 3.77; N, 5.96; P, 5.27; F, 14.56. Found: C, 50.64; H, 3.89; N, 5.85; P, 5.44; F, 15.28. Infrared spectrum (KBr pellet, cm^{-1}): ν(N=C=N) 1567 (s); $\nu_{asym}(CO)_2$ 1631 (s).

Synthesis of $[Rh_2(form)_2(\mu\text{-}PPh_2Py)_2(O_2CCF_3)]PF_6$ (4). Excess $TlPF_6$ was added to an acetone solution of **2** (0.15 g, 0.1 mmol). The resulting green solution was stirred at room temperature for 1 h and then filtered. The filtrate was taken to dryness and the green powder obtained extracted with benzene. The filtrate was taken to dryness and crystallized from CH_2Cl_2/*n*-heptane, giving green needles of **4**. Yield: 86%. Anal. Calcd for $C_{66}H_{58}N_6P_3O_2F_9Rh_2$: C, 55.17; H, 4.06; N, 5.84; P, 6.46; F, 11.89. Found: C, 55.55; H, 4.10; N, 5.96; P, 6.13; F, 11.73. Infrared spectrum (KBr pellet, cm^{-1}): ν(N=C=N) 1567 (vs); $\nu_{asym}(CO_2)$ 1684 (vs).

Synthesis of $[Rh_2(form)_2(\mu\text{-}PPh_2Py)_2][PF_6]_2$ (5). Crude $TlPF_6$ (0.07 g, 0.2 mmol) was added to a CH_3CN solution of **2** (0.15 g, 0.1 mmol). After 3 h the solution was filtered and taken to dryness. The solid obtained was crystallized twice from $CHCl_3$/*n*-heptane, giving complex **5**. Yield: 46%. Anal. Calcd for $C_{64}H_{58}N_6F_{12}P_4Rh_2$: C, 52.33; H, 3.98; N, 5.72; P, 8.43; F, 15.51. Found: C, 52.65; H, 3.96; N, 5.76; P, 8.18; F, 13.74. Infrared spectrum (KBr pellet, cm^{-1}): ν(N=C=N) 1562 (s).

Synthesis of $Rh_2(form)_2(\mu\text{-}O_2CCF_3)(\mu\text{-}PPh_2Py)Cl$ (6). The complex was prepared by refluxing for 6 h a benzene solution of **1** (0.13 g, 0.11 mmol) with an excess of KCl. The pink-red solution obtained was filtered and taken to dryness. The resulting solid was washed with diethyl ether and crystallized twice from $CHCl_3$/*n*-heptane. Yield: 63%. Anal. Calcd for $C_{49}H_{44}N_5F_3O_2ClPRh_2$: C, 55.30; H, 4.16; N, 6.58; P, 2.81; Cl, 3.33. Found: C, 54.89; H, 4.28; N, 6.88; P, 2.80; Cl, 2.89. IR spectrum (KBr pellet, cm^{-1}): ν(N=C=N) 1574 (2); $\nu_{asym}(CO_2)$ 1643 (s).

Synthesis of $Rh_2(form)_2(\mu\text{-}O_2CCF_3)(\mu\text{-}PPh_2Py)Br$ (7). This complex was prepared by reacting a CH_2Cl_2 solution of **1** (0.13 g, 0.11 mmol) with an excess of KBr at room temperature for 40 h. The solution was filtered and the solvent removed in vacuo. The green solid obtained was crystallized twice from CH_2Cl_2/*n*-heptane, giving green needles of complex **7**. Yield: 65%. Anal. Calcd for $C_{49}H_{44}N_5F_3O_2BrPRh_2$: C, 53.09; H, 4.0; N, 6.31; P, 2.79; Br, 7.20. Found: C, 52.89; H, 3.9; N, 5.89; P, 2.59; Br, 8.0. IR spectrum (KBr pellet, cm^{-1}): ν(N=C=N) 1565 (s); $\nu_{asym}(CO_2)$ 1634 (s).

Synthesis of $Rh_2(form)_2(\mu\text{-}PPh_2Py)_2(O_2CCF_3)Cl$ (8). Crude KCl (0.1 g, 0.86 mmol) was added to a stirred solution of **2** (0.15 g, 0.1 mmol) in CH_2Cl_2. After 15 h the supernatant solution had became green in color. After filtration, the solution was evaporated to dryness, and the residue was crystallized twice from CH_2Cl_2/*n*-heptane, giving red crystals. Yield: 85%. Anal. Calcd for $C_{66}H_{58}N_6P_2F_3ClO_2Rh_2$: C, 60.60; H, 4.82; N, 6.10; P, 4.49; Cl, 2.57. Found: C, 60.48; H, 4.70; N, 5.96; P, 4.35; Cl, 2.48. Infrared spectrum (KBr pellet, cm^{-1}): ν(N=C=N) 1553 (s), $\nu_{asym}(CO_2)$ 1684 (vs).

Synthesis of $Rh_2(form)_2(\mu\text{-}PPh_2Py)_2I_2$ (9). A solution of **2** in CH_2Cl_2 (0.15 g, 0.1 mmol) was treated with an excess of KI, and the heterogeneous mixture thus formed was stirred at room temperature for 3 h. During this time the solution changes to a green color. The mixture was filtered and taken to dryness, and the residue was crystallized twice from $CHCl_3$/*n*-heptane, giving green crystals. Yield: 78%. Anal. Calcd for $C_{64}H_{58}N_6P_2I_2Rh_2$: C, 53.65; H, 4.08; N, 5.86; P, 4.32; I, 17.71. Found: C, 53.78; H, 4.19; N, 5.80; P, 4.50; I, 17.42. Infrared spectrum (KBr pellet, cm^{-1}): ν(N=C=N) 1557 (vs).

X-ray Data and Structure Refinement. Suitable red-orange crystals of **2** were obtained by slow evaporation of the solvent from a dichloromethane/*n*-hexane solution. Diffraction measurements were made on a Syntex R3/m four-circle diffractometer using graphite-monochromated Mo Kα (λ = 0.710 73 Å) radiation. Cell dimensions were determined and refined with constraints by 25 accurately centered reflections having $14° < 2\theta < 26°$. The compound crystallizes in the monoclinic space group $P2_1/n$, with a = 19.608 (2) Å, b = 19.384 (2) Å, c = 20.576 (3) Å, β = 117.16 (3)°, V = 6958.34 Å^3, Z = 4, and d_c = 1.343 g/cm^3. During the course of the intensity data collection the crystals showed no loss in intensity. The reflections were corrected for Lorentz–polarization effects and extinction, the parameter of which was included in the final refinement cycles. No account was taken for the absorption correction because of the low absorption coefficient (μ = 5.5 cm^{-1}) and the fairly uniform dimensions of the crystals. Crystallographic data and other pertinent information are summarized in Table I and SI (supplementary material).

The structure was solved by using standard Patterson methods, successive least-squares refinements, and difference Fourier maps. Hydrogen atoms were added at calculated positions and included in the structure factor calculations with a common thermal parameter (U = 0.06 Å^2). The refinement converged to R = 0.056 and R_w = 0.065 with the goodness of fit S = 0.743 and was characterized by an 18:1 rate of

Table I. Crystallographic Data

formula	$C_{68}H_{60}F_6N_6O_4P_2Rh_2$	space group	$P2_1/n$ (No. 14)
fw	1407.02	T, °C	19
a, Å	19.608 (2)	λ, Å	0.71073
b, Å	19.384 (2)	d_c, g/cm^3	1.343
c, Å	20.576 (3)	μ, cm^{-1}	5.5
β, deg	117.16 (3)	R	0.056
V, Å^3	6958.34	R_w	0.065
Z	4		

observation per parameter. The weighting scheme used in the last refinement cycles was $w = 0.5934/(\sigma^2|F_o| + 0.008666|F_o|^2)$, which showed reasonable consistency in a test of $w\Delta^2$ for data sectioned with respect to both F_o and $(\sin\theta)/\lambda$.

Scattering factors for non-hydrogen atoms were taken from ref 5, and those for hydrogen atoms, from ref 6. Anomalous dispersion corrections for Rh and P atoms were taken from ref 7. All calculations were performed with the SHELX 76[8] and PARST[9] sets of programs on the IBM 3090/120S computer at the "Centro di Calcolo dell'Università di Messina". Full lists of bond distances and angles, hydrogen coordinates, anisotropic temperature factors, positional parameters, and calculated and observed structure factors are available as supplementary material.

Results

The Rh_2^{4+} complex $Rh_2(form)_2(O_2CCF_3)_2(H_2O)_2$ reacts with 1 equiv of 2-(diphenylphosphino)pyridine to give the complex $Rh_2(form)_2(\mu\text{-}O_2CCF_3)(\mu\text{-}PPh_2Py)(O_2CCF_3)$ (**1**). Once formed, complex **1** undergoes further reaction with an additional 1 equiv of PPh_2Py to rapidly generate the complex $Rh_2(form)_2(\mu\text{-}PPh_2Py)_2(O_2CCF_3)_2$ (**2**). Complex **2** can be straightforwardly obtained by reacting the parent complex with 2 equiv of PPh_2Py, and to confirm the stability of the Rh–(form)$_2$–Rh fragment, no further reaction occurs when an excess of ligand is used. Both new complexes are air-stable crystalline solids for which satisfactory analytical data have been obtained. The structure of **1** and **2** follows from their spectroscopic properties and conductivity measurements and for complex **2** from X-ray analysis.

The solid-state IR spectrum of complex **1** exhibits, in the 1600–1700-cm^{-1} region, absorptions at 1635 (vs), 1687 (m), and 1701 (m) cm^{-1}. The lower value is consistent with those of chelating or bridging fluorocarboxylate groups, while the higher values suggest the presence of monodentate or uncoordinated CF_3COO groups. On the contrary, the occurrence of a single ν(CO) band at 1663 cm^{-1} in the solid-state IR spectrum of complex **2** suggests, in accordance with the X-ray crystal structure, that both the trifluoroacetate groups are coordinated in a similar manner. However, solution IR spectra reveal that complexes **1** and **2** adopt in solution different configurations. In fact, the IR spectra of complex **2**, recorded in solvents such as benzene, chloroform, methanol, tetrahydrofuran, or acetone, display, in the 1600–1700-cm^{-1} region, only a broad absorption at 1683 cm^{-1}, while the spectra recorded in coordinating solvents such as CH_3CN or DMSO show absorptions at 1696 cm^{-1}. The solution IR spectrum of **1** seems little different from the solid one except for the spectrum recorded in CH_3CN or DMSO, which shows bands at 1635 and 1695 cm^{-1}.

On the other hand, molar conductivity measurements carried out on acetonitrile solutions of **2** (10^{-3} and 10^{-4} M) show unambiguously that complex **2** behaves as a 1:2 electrolyte, whereas in poorly or noncoordinating solvents, such as methanol, nitrobenzene, acetone, and dichloromethane complex, **2** is only partially dissociated, having the molar conductivity that one would expect for a 1:1 electrolyte. Complex **1** exhibits in acetonitrile solution (10^{-3} and 10^{-4} M) molar conductance values of 106 and 117 Ω^{-1} cm^2 mol^{-1}, respectively, indicating that **1** behaves as a 1:1 electrolyte. The values found in other solvents, such as nitrobenzene and dichloromethane, indicate that the complex is poorly dissociated. Conductivity and IR data may be interpreted in terms of dissociation of one or both the trifluoroacetate groups depending on the coordinating power of the solvents, so that the species operating in acetonitrile solution are $[Rh_2(form)_2(\mu\text{-}O_2CCF_3)(\mu\text{-}PPh_2Py)L_n]CF_3COO$ (L = CH_3CN; n = 0, 1) and $[Rh_2(form)_2(\mu\text{-}PPh_2Py)_2L_n][CF_3COO]_2$ (L = CH_3CN; n = 0, 1, 2), while in poorly coordinating solvents only one CF_3COO group

Table II. Selected Bond Distances (Å) and Angles (deg)

Distances			
Rh(1)–Rh(2)	2.5406 (6)	Rh(1)–O(1)	2.407 (4)
Rh(1)–N(1)	2.056 (5)	Rh(1)–N(3)	2.139 (4)
Rh(1)–P(1)	2.267 (1)	Rh(1)–N(6)	2.074 (5)
Rh(2)–O(3)	2.327 (4)	Rh(2)–N(2)	2.126 (6)
Rh(2)–N(4)	2.050 (4)	Rh(2)–N(5)	2.069 (4)
Rh(2)–P(2)	2.269 (2)	C(6)–C(5)	1.51 (1)
C(65)–O(1)	1.241 (9)	C(65)–O(2)	1.23 (1)
C(66)–F(1)	1.30 (2)	C(66)–F(2)	1.26 (1)
C(66)–F(3)	1.24 (1)	C(67)–C(68)	1.52 (1)
C(67)–O(3)	1.244 (8)	C(67)–O(4)	1.230 (8)
C(68)–F(4)	1.30 (1)	C(68)–F(5)	1.20 (2)
C(68)–F(6)	1.25 (1)	F(5)–F(6)	1.77 (3)
N(1)–C(1)	1.314 (8)	N(1)–C(2)	1.434 (6)
C(1)–N(2)	1.325 (6)	N(2)–C(9)	1.422 (9)
N(3)–C(16)	1.336 (8)	N(3)–C(17)	1.401 (8)
C(16)–N(4)	1.314 (8)	N(4)–C(24)	1.447 (7)
P(1)–C(31)	1.818 (6)	P(1)–C(37)	1.820 (8)
P(1)–C(43)	1.835 (5)	C(64)–N(6)	1.359 (8)
C(43)–N(5)	1.365 (7)	C(47)–N(5)	1.326 (7)
P(2)–C(48)	1.822 (5)	C(60)–N(6)	1.352 (7)
P(2)–C(54)	1.817 (6)	P(2)–C(60)	1.834 (6)
Angles			
P(1)–Rh(1)–N6)	91.5 (1)	N(3)–Rh(1)–N(6)	88.0 (2)
N(3)–Rh(1)–P(1)	170.0 (1)	N(1)–Rh(1)–N(6)	176.5 (2)
N(1)–Rh(1)–P(1)	92.0 (1)	N(1)–Rh(1)–N(3)	88.6 (2)
O(1)–Rh(1)–N(6)	93.7 (2)	O(1)–Rh(1)–P(1)	83.3 (1)
O(1)–Rh(1)–N(3)	106.7 (1)	O(1)–Rh(1)–N(1)	86.1 (2)
Rh(2)–Rh(1)–N(6)	96.0 (1)	Rh(2)–Rh(1)–P(1)	86.5 (4)
Rh(2)–Rh(1)–N(3)	83.5 (1)	Rh(2)–Rh(1)–N(1)	84.8 (1)
Rh(2)–Rh(1)–O(1)	166.1 (1)	Rh(1)–Rh(2)–P(2)	86.0 (4)
Rh(1)–Rh(2)–N(5)	96.3 (1)	Rh(1)–Rh(2)–N(4)	85.1 (1)
Rh(1)–Rh(2)–N(2)	83.5 (1)	Rh(1)–Rh(2)–O(3)	64.5 (1)
N(5)–Rh(2)–P(2)	92.1 (1)	N(4)–Rh(2)–P(2)	94.0 (1)
N(4)–Rh(2)–N(5)	73.8 (2)	N(2)–Rh(2)–P(2)	169.1 (1)
N(2)–Rh(2)–N(5)	86.1 (2)	N(2)–Rh(2)–N(4)	88.1 (2)
O(3)–Rh(2)–P(2)	84.8 (1)	O(3)–Rh(2)–N(5)	96.4 (2)
O(3)–Rh(2)–N(4)	83.1 (2)	O(3)–Rh(2)–N(2)	106.1 (2)
O(1)–C(65)–O(2)	130.5 (7)	C(66)–C(65)–O(2)	113.9 (6)
Rh(1)–O(1)–C(65)	150.1 (4)	Rh(2)–O(3)–C(67)	150.8 (4)
Rh(1)–N(1)–C(2)	122.1 (4)	Rh(1)–N(1)–C(1)	119.3 (4)
C(1)–N(1)–C(2)	118.3 (5)	N(1)–C(1)–N(2)	123.0 (6)
Rh(2)–N(2)–C(1)	115.3 (4)	Rh(1)–N(3)–C(17)	130.9 (4)
Rh(2)–N(2)–C(9)	127.6 (4)	N(1)–C(2)–C(8)	121.6 (5)
N(1)–C(2)–C(3)	120.7 (5)	C(3)–C(2)–C(8)	117.7 (5)
Rh(1)–N(3)–C(16)	112.9 (3)	Rh(1)–P(1)–C(31)	114.3 (2)
N(3)–C(16)–N(4)	124.1 (5)	Rh(2)–N(4)–C(16)	119.0 (4)
C(16)–N(4)–C(24)	116.6 (4)	Rh(2)–N(4)–C(24)	124.4 (3)
P(1)–C(43)–N(5)	117.0 (4)	P(2)–C(60)–N(6)	116.0 (5)
Rh(2)–P(2)–C(60)	111.8 (2)	Rh(2)–P(2)–C(54)	120.0 (2)
Rh(2)–P(2)–C(48)	116.3 (2)	Rh(1)–N(6)–C(60)	122.9 (4)
Rh(1)–N(6)–C(64)	120.2 (4)		

Table III. Non-Hydrogen Atom Coordinates with Esd's in Parentheses

atom	x/a	y/b	z/c
Rh(1)	0.22028 (2)	0.17154 (2)	0.00913 (2)
Rh(2)	0.22911 (2)	0.29201 (2)	−0.03509 (2)
O(1)	0.2211 (2)	0.0491 (2)	0.0289 (2)
O(3)	0.2444 (3)	0.4102 (2)	−0.0435 (2)
N(1)	0.3270 (2)	0.1576 (2)	0.0152 (2)
N(2)	0.3033 (3)	0.2435 (2)	−0.0709 (2)
N(3)	0.2743 (3)	0.2188 (2)	0.1147 (2)
N(4)	0.3218 (3)	0.3038 (2)	0.0654 (2)
P(1)	0.16113 (8)	0.14056 (7)	−0.11024 (7)
N(5)	0.1439 (2)	0.2788 (2)	−0.1410 (2)
P(2)	0.14297 (8)	0.32303 (7)	0.00471 (7)
N(6)	0.1159 (2)	0.1863 (2)	0.0099 (2)

(5) Cromer, D. T.; Mann, J. B. *Acta Crystallogr., Sect. A* **1968**, *24*, 321.
(6) Stewart, R. F. *J. Chem. Phys.* **1970**, *53*, 3175.
(7) *International Tables for X-ray Crystallography*; Kynoch Press: Birmingham, England, 1974; Vol. IV.
(8) Sheldrick, M. G. System of Computing Programs. University of Cambridge, 1976.
(9) Nardelli, M. *Comput. Chem.* **1983**, *7*, 95.

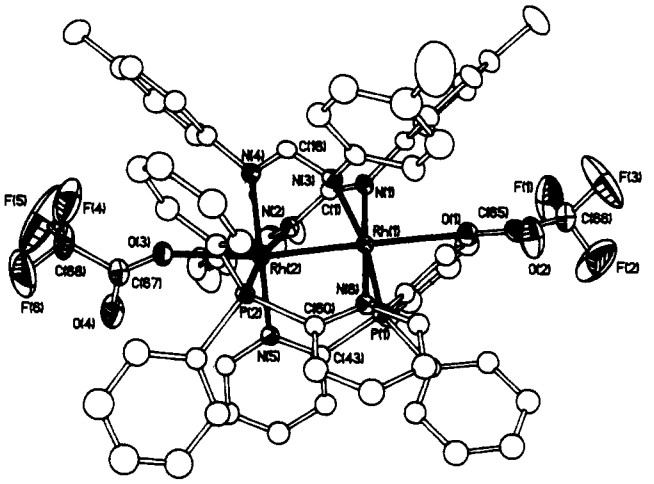

Figure 1. Molecular structure of $Rh_2(form)_2(\mu\text{-}PPh_2Py)_2(O_2CCF_3)_2$ (**2**). Dashed ellipsoids and labels are indicated only for the atoms involved in the coordination geometry of the metallic centers and for the O_2CCF_3 groups. Thermal ellipsoids are drawn at 30% probability.

of complex **2** undergoes dissociation, giving the species $[Rh_2(form)_2(\mu\text{-}PPh_2Py)_2(O_2CCF_3)]CF_3COO$.

Discussion

Description of the Molecular Structure of $Rh_2(form)_2(\mu\text{-}PPh_2Py)_2(O_2CCF_3)_2$. The molecular structure of **2**, including the atomic numbering scheme, is illustrated in Figure 1. Selected bond distances and angles are listed in Table II. Final positional parameters are reported in Table III. The structure consists of two d^7 rhodium atoms at a bonding distance of 2.5406 (6) Å symmetrically bridged by two 2-(diphenylphosphino)pyridine ligands arranged in a cisoid, heat-to-tail fashion and two formamidinate groups. Two monoligated trifluoroacetate groups, located at the axial positions, complete the coordination of the metal centers. The geometry around Rh(1) and Rh(2) is a distorted octahedron with the N(form)–Rh–N(form) [mean value 88.4 (2)°], N(form)–Rh–N(Py) [mean value 87.1 (2)°], and N(form)–Rh–P [mean value 93.0 (1)°] angles different from 90°. The steric requirements and the different "bites" of the bridging ligands appear responsible for the above distortion.

The Rh–Rh bond length, which lies at the top of the range of distances observed in tetrabridged Rh_2^{4+} complexes, is longer than that found in the analogous complex $Rh_2(O_2CCH_3)_2(\mu\text{-}PPh_2Py)_2Cl_2$ [2.518 (1) Å],[10] and the difference of 0.032 Å may be ascribed to the different steric and electronic properties of the formamidinate and acetate ligands rather than to the axial substituents. The considerable lengthening of the Rh–Rh bond with respect to other dirhodium(II) derivatives is consistent with the presence of the PPh_2Py ligand. The Rh–Rh separation ranges from 2.4336 (4) to 2.5406 Å on going from $Rh_2(form)_4$[11] to **2** and from 2.3855 (5) to 2.518 (1) Å on going from $Rh_2(O_2CCH_3)_4$[12] to $Rh_2(O_2CCH_3)_2(PPh_2Py)_2Cl_2$.[10]

The Rh(1)–N(1) and Rh(2)–N(4) distances [mean value 2.062 (4) Å] are comparable with the values found in related complexes in which the nitrogen atoms are in a trans position to each other,[11] while the lengthening of the other Rh–N(form) bonds reflects the trans influence of the phosphorus atoms. Also, the elongation of the Rh–P bonds [mean value 2.268 (1) Å] with respect to those of $Rh_2(O_2CCH_3)_2(PPh_2Py)_2Cl_2$ [mean value 2.21 (2) Å] reflects the influence of the trans nitrogen. The structural features of the bridging PPh_2Py and formamidinate ligands are essentially the same as observed in the previously cited complex and other formamidinate derivatives. All the bridging ligands are not planar with averaged values of 19.7 and 26.8° for the N–Rh–Rh–P and N–Rh–Rh–N torsion angles, respectively.

Table IV. ^{31}P Chemical Shifts (ppm) and Coupling Constants (Hz) in $CDCl_3$

complex	temp, K	$\delta(^{31}P)$	$^1J_{P-Rh}$	$^2J_{P-Rh}$
1	225	−34.36	82.8	55.4
	310	30.21	127.0	5.7
		29.53	126.4	5.3
	310 (CD_3CN)	30.9	127.6	3.3
2	225	−96.05		
	310	29.01	132	
	310 (CD_3CN)	25.83	129.7	
3	310	29.68	122.2	5.2
4	310	26.8	127.1	
5	310	28.74	131.1	
6	225	24.35	164.5	5.8
7	310	28.79	122.2	5.4
8	310	27.90	131.3	
9	310	27.82	129.9	

The trifluoroacetate groups are bonded to the rhodium atoms with different Rh–O distances and are bent away from the bulky phosphine groups. The Rh–Rh–O angles deviate significantly from linearity [166.2 (1) and 164.5 (1)°], indicating strong steric interactions between the trifluoroacetate groups and the bridging ligands. The interactions involving O(2), O(2)···C(64) = 3.208 Å and O(2)···C(18) = 3.288 Å, and O4, O(4)···C(47) = 3.047 Å, may be regarded as hydrogen bonds as well as the intermolecular O(2)···C(34) and O(4)···C(40) interactions at 3.220 and 3.255 Å, respectively.

Generation and Spectral Characterization of Complexes 1 and 2. The reaction sequence leading to complexes **1** and **2** was monitored by ^{31}P NMR spectroscopy to provide information about the mechanism operating during the formation of **1** and **2**. The complexes **1** and **2** have been generated at room temperature in a ^{31}P NMR tube by adding, via a syringe, the appropriate amount of ligand, dissolved in $CDCl_3$, to a solution of $Rh_2(form)_2(O_2CCF_3)_2(H_2O)_2$ dissolved in the same solvent; immediately after the reaction mixture was cooled at 225 K.

The ^{31}P NMR spectrum recorded at 225 K reveals the quasi-quantitative formation of a 1:1 adduct together with a doublet of doublets centered at δ −34.46 with two large coupling constants ($^1J_{P-Rh}$ = 82.8 Hz; $^2J_{P-Rh}$ = 55.4 Hz) (Table IV). These values are consistent with the formation of a 1:1 adduct with a linear arrangement of the Rh–Rh–P atoms (class I) and compare well with those found for similar complexes.[1] The spectrum also shows a week triplet centered at δ −96.05, which is likely to be due to a 1:2 bisaxial adduct. The triplet, according to what found for the complex $Rh_2(O_2CCH_3)_4[P(OMe)_3]_2$,[13] is interpreted as the X portion of an AA′XX′ spin system where the linear arrangement of the P–Rh–Rh–P fragment allows a very strong PP′ coupling across the dirhodium core.

The monoaxial adduct is stable at 225 K, but on warming to 310 K, it rapidly rearranges to form a mixture of isomers (Figure 2) whose chemical shifts and J_{P-Rh} coupling constants lie in the range quoted for Rh_2^{4+} equatorial adducts (class II).[1,14]

The ^{31}P NMR spectrum at 310 K shows two pairs of doublets, one broad, centered at δ 30.21 ($^1J_{P-Rh}$ = 127.0 Hz; $^2J_{P-Rh}$ = 5.7 Hz), the other one sharp, centered at δ 29.53 ($^1J_{P-Rh}$ = 126.4 Hz; $^2J_{P-Rh}$ = 5.3 Hz). The conversion of the linear to the bent Rh–Rh–P is irreversible: upon cooling of the sample to 225 K the ^{31}P NMR spectra show a marked sharpening of the signal centered at δ 30.29, while there is no back-transformation of the equatorial isomers into axial adducts.

The broadness of the resonance centered at δ 30.29 suggests that some dynamic process is operating at room temperature, but its nature as well as the geometry of these isomers is so far uncertain. However, we suspect that the isomerization of the axial to the equatorial isomer occurs through a mechanism similar to

(10) Cotton, F. A.; Matusz, M. *Inorg. Chim. Acta* **1988**, *143*, 45.
(11) Piraino, P.; Bruno, G.; Lo Shiavo, S.; Laschi, F.; Zanello, P. *Inorg. Chem.* **1987**, *26*, 2205.
(12) Cotton, F. A.; DeBoer, B. G.; La Prade, M. D.; Pipal, J. R.; Ucko, D. A. *J. Am. Chem. Soc.* **1970**, *92*, 2996.
(13) Boyar, E. B.; Robinson, S. D. *Inorg. Chim. Acta* **1982**, *64*, L193.
(14) Piraino, P.; Bruno, G.; Tresoldi, G.; Lo Schiavo, S.; Nicolò, F. *Inorg. Chem.* **1989**, *28*, 139. (b) Telser, J.; Drago, R. S. *Inorg. Chem.* **1986**, *25*, 2992.

Scheme II

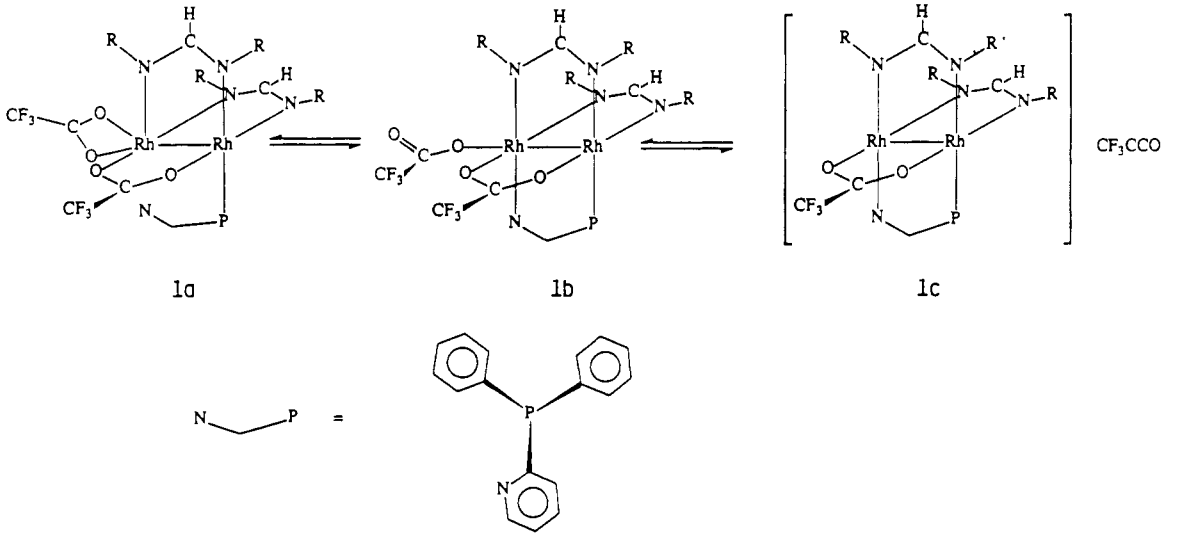

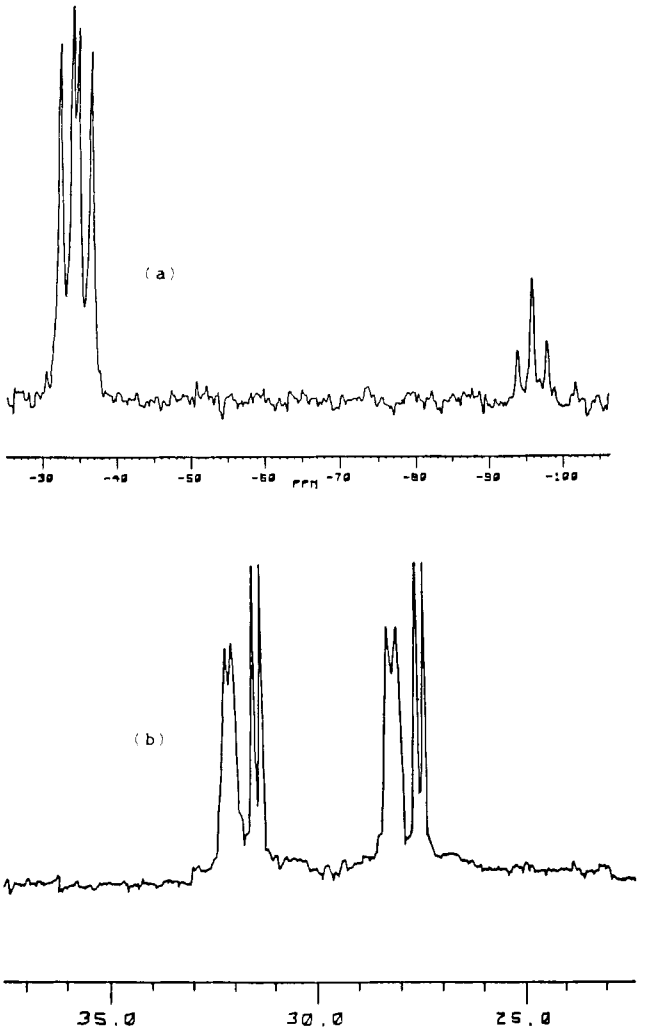

Figure 2. ^{31}P NMR spectra of $Rh_2(form)_2(\mu\text{-}O_2CCF_3)(\mu\text{-}PPh_2Py)(O_2CCF_3)$ (**1**) in $CDCl_3$: (a) at 225 K; (b) at 310 K.

that depicted in Scheme I. Once formed, species **1a** undergoes ring closure of the Rh–Rh–P–N fragment and formation of the species **1b** (Scheme II).

The sharp signal centered at δ 29.53 may be ascribed to the species **1a**, while the broadness of the second doublet may arise from a fast reversible dissociation of one trifluoroacetate group with formation of the species **1c**. The equilibrium between **1a** and **1b** is slow on the NMR time scale even at 310 K, while the equilibrium between **1b** and **1c** implies for these species at 310 K half-lives of the same order of magnitude as the NMR time scale. This suggestion is consistent with the presence in the ^{31}P NMR spectrum of a doublet of doublets centered at δ 29.53 that is sharp both at 310 and 225 K, while the second doublet of doublets centered at δ 30.21 is sharp at 225 K and becames broad at 310 K.

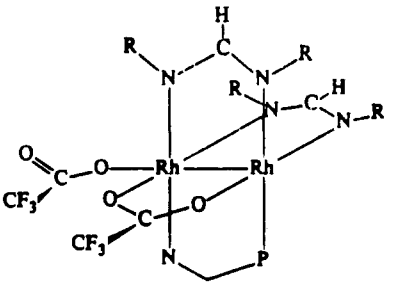

Figure 3. Proposed solid-state structure of **1**.

Consistent with the proposed mechanism are conductivity and IR data (see before). When the experiment is performed in CD_3CN, the ^{31}P NMR spectrum at 310 K shows only a sharp double doublet centered at δ 30.9 ($^1J_{P\text{-}Rh}$ = 127.6 Hz; $^2J_{P\text{-}Rh}$ = 3.3 Hz). This resonance may be ascribed to the monocationic species **1c**, indicating that in CD_3CN the equilibrium depicted in Scheme II is shifted toward the right.

Although the structure of complex **1** cannot be assigned unambiguously, we suggest, on the basis of the evidence gathered, that it adopts in the solid state a configuration closely related to that found for complex **2** (Figure 3).

The reaction was also performed with different molar ratios, namely 1:2 and 1:4. In both cases the ^{31}P NMR spectra, recorded in $CDCl_3$ at 225 K, reveal the quantitative formation of a bisaxial adduct exhibiting only the triplet centered at δ −96.05. The large low-frequency shift of the phosphorus resonance may indicate that each phosphorus atom, axially coordinated to the rhodium, is also involved in a four-membered chelating ring.[15] The reaction pattern could involve sequential axial coordination of the 2-(diphenylphosphino)pyridine ligands through the phosphorus atoms with formation of the classical bisadducts followed or not by chelation of the pyridine nitrogen atoms. Chelating behavior of the PPh_2Py ligand, although rare, is not unknown.[16]

On warming to 310 K, the bisaxial adduct slowly isomerizes to give the equatorial isomer **2**. The spectrum of **2** at 310 K exhibits a broad doublet centered at δ 29.01 ($^1J_{P\text{-}Rh}$ = 132 Hz), which remains unchanged upon cooling the mixture at 225 K. The presence of a doublet for the X part of the AA′XX′ spin system

(15) Garrou, P. E. *Chem. Rev.* **1981**, *81*, 229.
(16) Olmstead, M.; Maisonnat, A.; Farr, S. P.; Balch, A. L. *Inorg. Chem.* **1981**, *20*, 4060.

may be due to long-range couplings, as recently suggested by Tortorelli for the Rh_2^{4+} complexes $Rh_2(\mu\text{-}PPh_2Py)_2(CO)_2Cl_4$ and $[Rh_2(\mu\text{-}PPh_2Py)_2(t\text{-}BuNC)_2Cl_3]PF_6$.[17]

In order to obtain some evidence for the proposed solution structure, complexes **1** and **2** were allowed to react with $TlPF_6$. The products of the reaction of **1** and **2** with $TlPF_6$ are critically dependent on the solvent used. Complex **1** reacts with an excess of $TlPF_6$ in CH_3CN leading to the monocationic complex $[Rh_2(form)_2(\mu\text{-}O_2CCF_3)(\mu\text{-}PPh_2Py)]PF_6$ (**3**) whereas no reaction occurs when acetone is used as solvent. Complex **3** has been characterized by IR, ^{31}P NMR, and conductivity measurements. The solid-state IR spectrum of **3**, besides the ν(P-F) stretching, shows a single $\nu_{asym}(CO_2)$ at 1631 cm^{-1}, while the ^{31}P NMR spectrum exhibits the familiar double doublet, which is sharp both at 225 and 310 K. On the contrary, complex **2** reacts with $TlPF_6$ in acetone as solvent, affording the monocationic complex $[Rh_2(form)_2(\mu\text{-}PPh_2Py)_2(O_2CCF_3)]PF_6$ (**4**). The solid-state IR spectrum of **4** shows the expected ν(P-F) stretching as well as a band at 1684 cm^{-1}, indicating the presence of a monocoordinated carboxylate group. With a repeat of the synthesis in CH_3CN, the non-carboxylate compound $[Rh_2(form)_2(\mu\text{-}PPh_2Py)_2][PF_6]_2$ (**5**) was obtained, as shown by the IR spectrum, which does not show absorptions attributable to the ν(O-C-O) stretching frequency.

Both complexes **1** and **2** serve as convenient precursors to new Rh_2^{4+} complexes. They undergo metathetical exchange reactions in which one or both the monoligated trifluoroacetate groups are replaced by X^- ligands (X = Cl, Br, I). Treatment of **1** with an excess of KX (X = Cl, Br) produces the complexes $Rh_2(form)_2(\mu\text{-}O_2CCF_3)(\mu\text{-}PPh_2Py)X$ (X = Cl (**6**), Br (**7**)), while treatment of **2** with the same halides gives the complexes $Rh_2(form)_2(\mu\text{-}PPh_2Py)_2(O_2CCF_3)Cl$ (**8**) and $Rh_2(form)_2(\mu\text{-}PPh_2Py)_2I_2$ (**9**). Analytical data and IR spectroscopy provide excellent evidence of the displacement of the fluoro carboxylate groups. IR spectra of complexes **6** and **7** display $\nu(CO_2)$ absorptions at 1643 and 1634 cm^{-1}, strongly suggesting that only bridging or chelating trifluoroacetate groups are present, while in the spectra of **9** no bands attributable to the $\nu(CO_2)$ stretching are present.

Acknowledgment. We thank the Public Ministry of Education for financial support.

Supplementary Material Available: Tables SI-SVII, listing full crystal data, nonessential atomic distances and angles, hydrogen atom parameters, temperature factors, and complete positional parameters, and a figure showing a packing diagram (10 pages); a table of calculated and observed structure factors (59 pages). Ordering information is given on any current masthead page.

(17) Woods, C.; Tortorelli, L. J. *Polyhedron* **1988**, *7*, 1751.

Contribution from the Departments of Chemistry, University of South Alabama, Mobile, Alabama 36688, and Auburn University, Auburn, Alabama 36849

Synthesis and Reactivity of Carbonylbis(triphenylphosphine)rhodium(I) Complexes of Water and Weakly Coordinating Anions

Daniel M. Branan,[†] Norris W. Hoffman,*[,†] E. Andrew McElroy,[†] Nicholas Prokopuk,[†] Anna B. Salazar,[†] Martha J. Robbins,[†] W. E. Hill,[‡] and Thomas R. Webb[‡]

Received October 19, 1989

New complexes *trans*-$Rh(PPh_3)_2(CO)OPOF_2$ and $[trans\text{-}Rh(PPh_3)_2(CO)(OH_2)]Z\cdot nH_2O$ (Z = SO_3CF_3, n = 1; Z = BF_4, n = 2; Z = ClO_4, n = 2) were prepared and characterized. Syntheses of the four species entailed metathesis of the Rh(I) chloride with $AgPF_6$, $AgSO_3CF_3$, $AgBF_4$, and $AgClO_4$, respectively, in undried solvents. The water-free $OPOF_2$ complex arises from hydrolysis of a spectroscopically detected Rh(I) PF_6^- species. Metathesis studies with $[N(PPh_3)_2]^+$ salts and reactions with pyridine and CO showed the affinity of $[Rh(PPh_3)_2(CO)]^+$ in CH_2Cl_2 for ligands L to follow the trend L = $(O_2CCF_3)^- > (ONO_2)^- >$ pyridine $> (OPOF_2)^- \gg H_2O \gg (SO_3CF_3)^- \approx (BF_4)^- \approx (ClO_4)^-$. Monoolefins such as C_2H_4 and $PhCH{=}CH_2$ failed to displace the very weakly coordinating ligand H_2O from $[Rh(PPh_3)_2(CO)(OH_2)]SO_3CF_3\cdot H_2O$ in CH_2Cl_2. The crystal structure of $[Rh(PPh_3)_2(CO)(OH_2)][BF_4]\cdot{}^1/_2H_2O\cdot{}^1/_4C_6H_{12}$ has been determined. The crystal belongs to the triclinic crystal system, space group $P\bar{1}$, with lattice constants a = 11.865 (2) Å, b = 17.235 (6) Å, c = 18.590 (5) Å, α = 91.95 (2)°, β = 101.62 (2)°, γ = 101.83 (2)°, and Z = 4.

Introduction

In the course of preparing a series of bis(triphenylphosphine)carbonylrhodium(I) complexes of uninegative ligands,[1,2] we became concerned about using $AgClO_4$ and the Rh(I) perchlorate complex[3] intermediate routinely.[4] We then tried readily available Ag^+ salts of several other weakly coordinating anions to effect similar metathesis of the chloride ligand to obtain a convenient synthon. Although we achieved the latter objective, we discovered that the actual products were not the results of the expected simple metathesis. Indeed, we found that the SO_3CF_3, BF_4, and ClO_4 complexes contained coordinated water (in addition to water of crystallization) rather than anionic ligand and the expected PF_6 complex had undergone hydrolysis in undried solvent to afford coordinated $(OPOF_2)^-$. [The synthesis of $Rh(PPh_3)_2(CO)(OSO_2CF_3)$ was reported while this study was in progress.[5]] To expand the ligand affinity data for $[Rh(PPh_3)_2(CO)]^+$ gathered earlier, we included the known nitrate and trifluoroacetate complexes (since $(O_2CCF_3)^-$ and $(ONO_2)^-$ are considered borderline weakly coordinating anions) along with the new difluorophosphate complex and the aqua cation in equilibrium studies of ligand substitution employing $[N(PPh_3)_2]^+$ salts and pyridine. We also studied the degree of displacement of anion or aqua ligand for the series with CO at 1 atm and for the aqua-$(SO_3CF_3)^-$ species with a set of alkenes.

Transition-metal complexes of weakly coordinating anions are of considerable interest as Lewis acid reagents,[6] and numerous

[†] University of South Alabama.
[‡] Auburn University.

(1) Araghizadeh, F.; Branan, D. M.; Hoffman, N. W.; Jones, J. H.; McElroy, E. A.; Miller, N. C.; Ramage, D. L.; Salazar, A. B.; Young, S. H. *Inorg. Chem.* **1988**, *27*, 3752.
(2) Branan, D. M.; Hoffman, N. W.; McElroy, E. A.; Eyler, J. R.; Watson, C. H.; deFur, P.; Leary, J. A. *Inorg. Chem.* **1990**, *29*, 1915.
(3) (a) Peone, J.; Vaska, L. *Angew. Chem., Int. Ed. Engl.* **1971**, *10*, 511. (b) Peone, J.; Vaska, L. *Inorg. Synth.* **1974**, *15*, 68.
(4) Cf.: *J. Chem. Educ.* **1973**, *50*, A335. *Chem. Eng. News* **1983**, *61* (Dec 5), 4; **1963**, *41* (July 8), 47.
(5) Liston, D. J.; Young, J. L.; Scheidt, R. W.; Reed, C. A. *J. Am. Chem. Soc.* **1989**, *111*, 6643.
(6) Two leading references: (a) Raab, K.; Beck, W. *Chem. Ber.* **1974**, *117*, 3169. (b) Cutler, A. R.; Todaro, A. B. *Organometallics* **1988**, *7*, 1782.

0020-1669/91/1330-1200$02.50/0